

Dehydrative Etherification Reactions of Glycerol with Alcohols Catalyzed by Recyclable Nanoporous Aluminosilicates: Telescoped Routes to Glyceryl Ethers

*Thomas E. Davies^a, Simon A. Kondrat^b, Ewa Nowicka^b, James J. Graham^c, David. C. Apperley^d,
Stuart. H. Taylor^b and Andrew E. Graham^{c*}*

^a Stephenson Institute for Renewable Energy, Department of Chemistry, University of Liverpool, L69
7ZD, UK

^b Cardiff Catalysis Institute, School of Chemistry, Cardiff University, Main Building, Park Place,
Cardiff, CF10 3AT, UK;

^b School of Applied Sciences, University of South Wales, CF37 4AT, UK;

^c EPSRC Solid-State NMR Service, Department of Chemistry, Durham University, DH1 3LE, UK;

*Corresponding author. Email: andrew.graham@southwales.ac.uk

Supplementary Information

Table of Contents

General Methods	S-2
Catalyst Characterization Methods	S-2
Catalyst Testing and Product Analysis	S-3
Catalyst Characterisation	
Figure S1: Al-13-(3.18) BET Isotherm Data	S-4
Figure S2: Al-13-(3.18) NLDTF Pore Size Distribution	S-5
Figure S3: Al-13-(3.18) XRD data	S-6
Figure S4a: Al-13-(3.18) ²⁷Al MAS NMR	S-7
Figure S4b: Al-13-(3.18) ²⁹Si MAS NMR	S-8
Figure S5: Al-13-(3.18) TPD Data	S-9
GC–MS Chromatograms	
Figure S6: GC–MS Chromatogram of the Reaction of Glycerol with PMBA (2:1) Catalyzed by Al-13-(3.18) in DMC	S-10
Figure S7: GC–MS Chromatogram of the Reaction of Glycerol with PMBA (2:1) Catalyzed by Amberlyst-15 in DMC	S-11
Figure S8: GC–MS Chromatograms of Telescoped Reactions of Glycerol with PMBA (4:1) catalyzed by Al-13-(3.18) in Acetone	S-12
Figure S9: GC–MS Chromatogram of Sequential Reaction of Glycerol with PMBA (4:1) catalyzed by Amberlyst-15 in Acetone	S-13
Figure S10: GC–MS Chromatogram of Crude Reaction of Glycerol with tert-BuOH catalyzed by Al-13-(3.18)	S-14
Spectroscopic Data for Ether Products	S-15
References	S-17

General Methods

Commercially available reagents were used without further purification. Infra-red (IR) spectra were recorded in the range 4000–600 cm^{-1} as neat oils or solids and are reported in cm^{-1} . Nuclear magnetic resonance (NMR) spectra were recorded at 400 MHz in CDCl_3 or DMSO-d_6 at 25 °C and are reported in ppm; J values are recorded in Hz and multiplicities are expressed by the usual conventions. Low-resolution mass spectra (MS) were determined by electron impact ionization (EI). High resolution mass spectra (HRMS) were obtained courtesy of the EPSRC Mass Spectrometry Facility, Swansea University, UK. Removal of solvent refers to evaporation at reduced pressure using a rotary evaporator followed by the removal of trace volatiles using a vacuum pump. Silicate, aluminosilicate and borosilicate samples were produced as described previously.¹⁻⁴ The commercial zeolite materials were purchased in their NH_4^+ form and calcined at 500 °C for 3 hours to provide the H^+ form. All catalysts were stored at 120 °C for at least 12 hours prior to use unless otherwise stated.

Catalyst Characterization Methods

Specific surface areas were obtained by the BET method at liquid nitrogen temperatures using a Micromeritics Gemini or a Quantachrome Autosorb-1 automated gas sorption instrument. Samples were degassed at 120 °C under a flow of helium for 2 hours prior to analysis. Pore sizes were obtained using a Quantachrome Autosorb-1 automated gas sorption instrument. Samples were degassed at 120 °C under vacuum for 3 hours prior to analysis. Pore sizes were calculated by applying the non-local density functional theory (NLDFT) method to the N_2 sorption at -196 °C employing Quantachrome AS-1 software data reduction parameters. Low angle XRD patterns were obtained using a Panalytical X'Pert Pro diffractometer. Measurements were performed in transmission mode at room temperature using monochromatic $\text{CuK}\alpha 1$ radiation. TEM analysis was performed on a Jeol 2100 operated at 200 kV. Samples were prepared by dispersion in methanol by sonication and deposited onto lacey carbon coated 300 mesh copper grids. ATR FT-IR spectra were obtained using a Perkin Elmer Spectrum Two spectrometer. NH_3 -TPD experiments were carried out using a Quantachrome ChemBet TPR/TPD Chemisorption Analyser. Prior to the measurements, approximately 30 mg of sample was activated by heating at 100 °C for 1 h. The sample was then

cooled to room temperature before treating with ammonia for 30 minutes. Physically adsorbed ammonia was removed by purging with helium at 90 °C for 1 hour before the NH₃-TPD analysis. The NH₃-TPD of the samples was carried out by increasing the cell temperature linearly from 90 °C to 900 °C with a heating rate of 20 °C min⁻¹ and a helium flow rate of 80 cm³ min⁻¹. Elemental compositions were obtained with a JOEL scanning electron microscope fitted with an EDX detector using a 20 KeV accelerating voltage. MAS-NMR spectra were obtained courtesy of the EPSRC National Solid State NMR Service, Durham University. Aluminium spectra were obtained using a Varian VNMRs system, with direct excitation (DE) and the results are reported relative to an external 1M aqueous Al(NO₃)₃ solution. Silicon spectra were obtained using a Varian Unity Inova spectrometer with a DE or cross polarisation (CP) from protons and the results are reported in ppm with respect to neat tetramethylsilane. Boron spectra were obtained using a Varian VNMRs system and results are reported relative to external BF₃·Et₂O.

Catalyst Testing and Product Analysis

All reactions were carried out in a sealed batch reactor. The catalyst was removed from the sample by filtration through a Celite plug, which was washed with DMC (2 × 2 mL) and the combined solvents were removed under reduced pressure. Product mixtures were analysed using ¹H NMR and GC–MS techniques, and percentage conversions of reactions were determined by integration of the relevant signals from crude ¹H NMR spectra.⁵⁻¹¹ Percentage conversions of reactions involving glycerol with TBA were determined from ¹H NMR spectra carried out in DMSO-d₆ by integration of the 2-hydroxy group (δ = 4.5) and *tert*-butyl group (δ = 1.15). For telescoped reaction procedures, percentage conversions were determined from integration of the isopropylidene methyl signals of solketal and the relevant alkylated solketal products.^{6,9-11} Product distributions from telescoped reactions involving PMBA and TBA were also determined by GC analysis employing an FID detector. These samples were analysed using a Varian Star 3800 Cx GC employing a 30m CP-Wax 52 CB column. GC–MS analysis was performed using a Varian 450GC and Varian 300MS employing a VF-5ms capillary column (30m, 0.25mm i.d. and 0.25 μ m) and a gradient temperature profile with an initial temperature of 50 °C for 3 minutes rising to 280 °C at a rate of 20 °C min⁻¹.

Figure S1: Al-13-(3.18) BET Isotherm

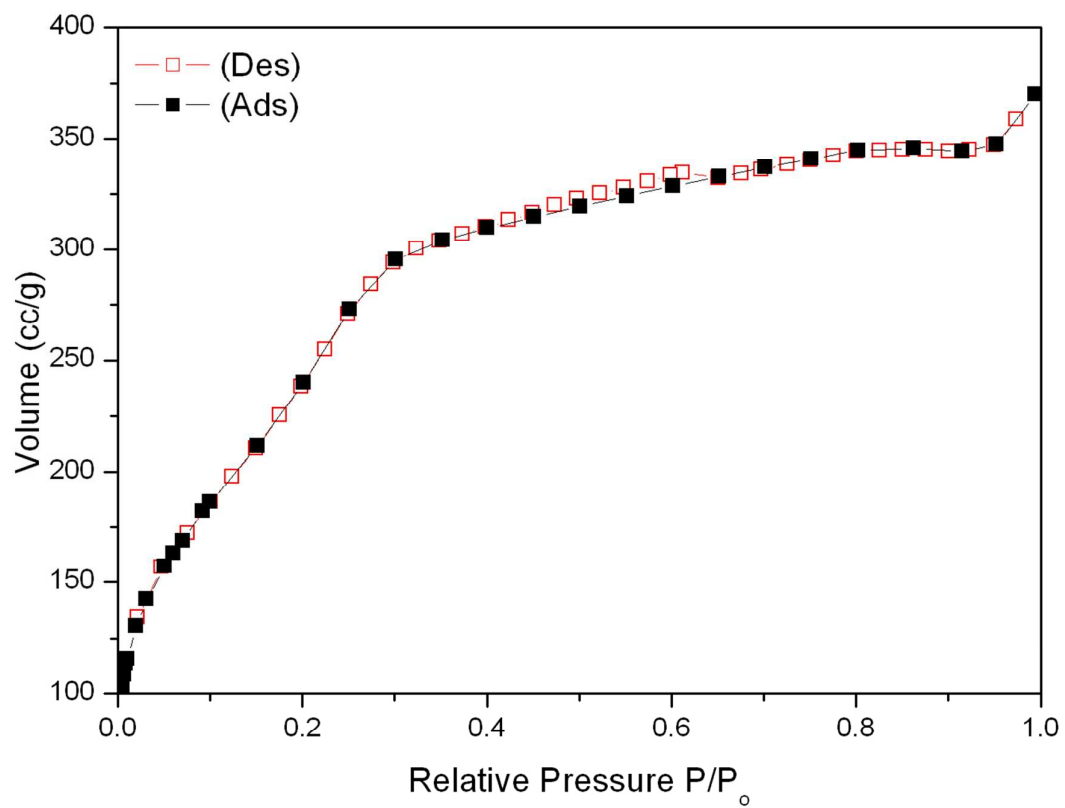


Figure S2: Al-13-(3.18) NLDFT Pore Size Distribution

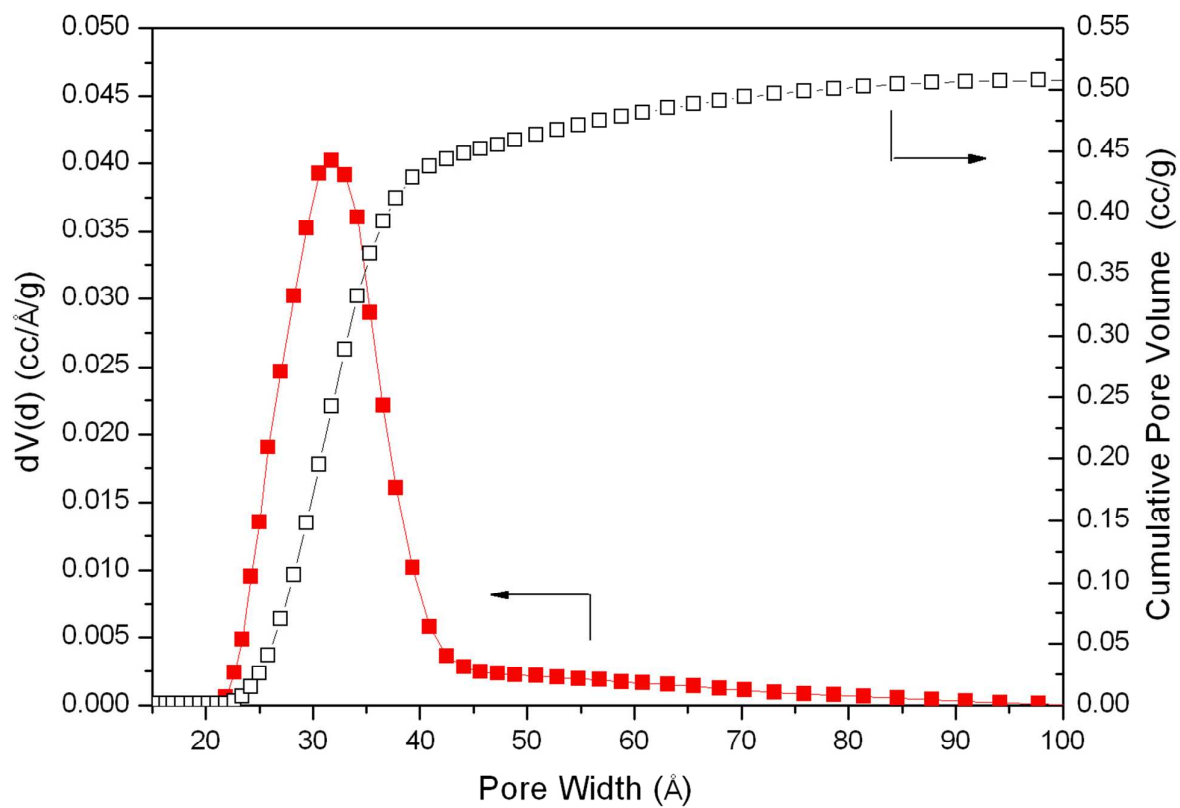


Figure S3: Al-13-(3.18) XRD Data

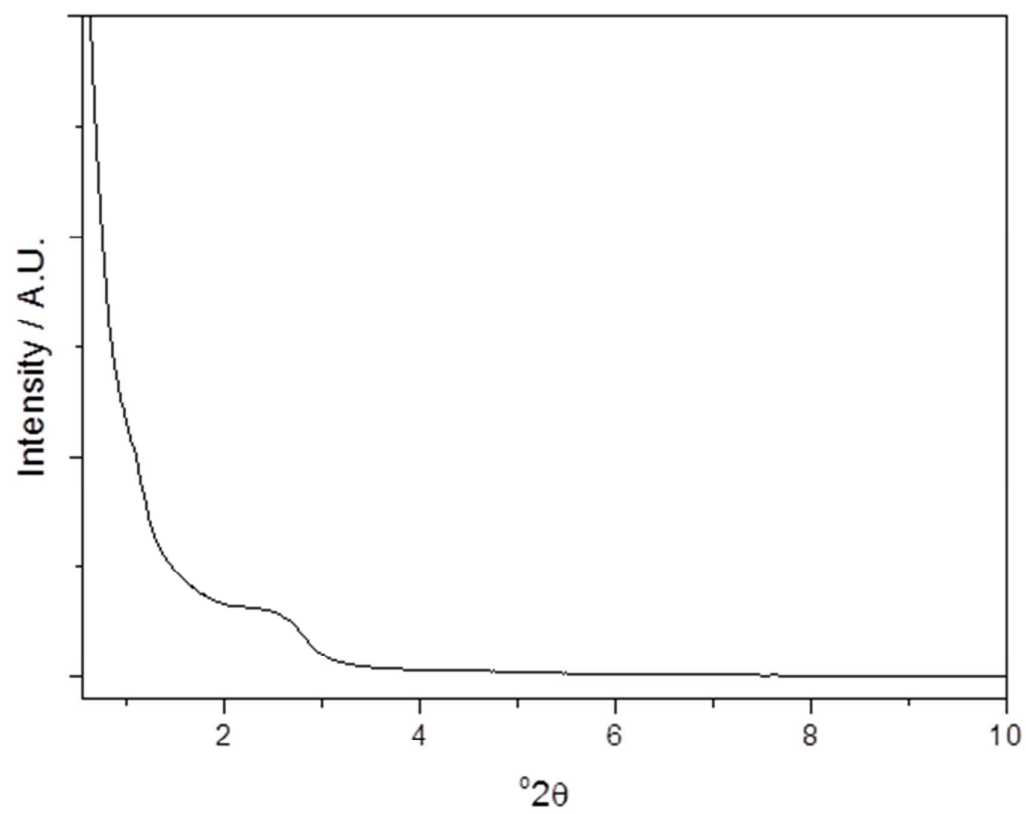


Figure S4a: ^{27}Al MAS NMR Al-13-(3.18)

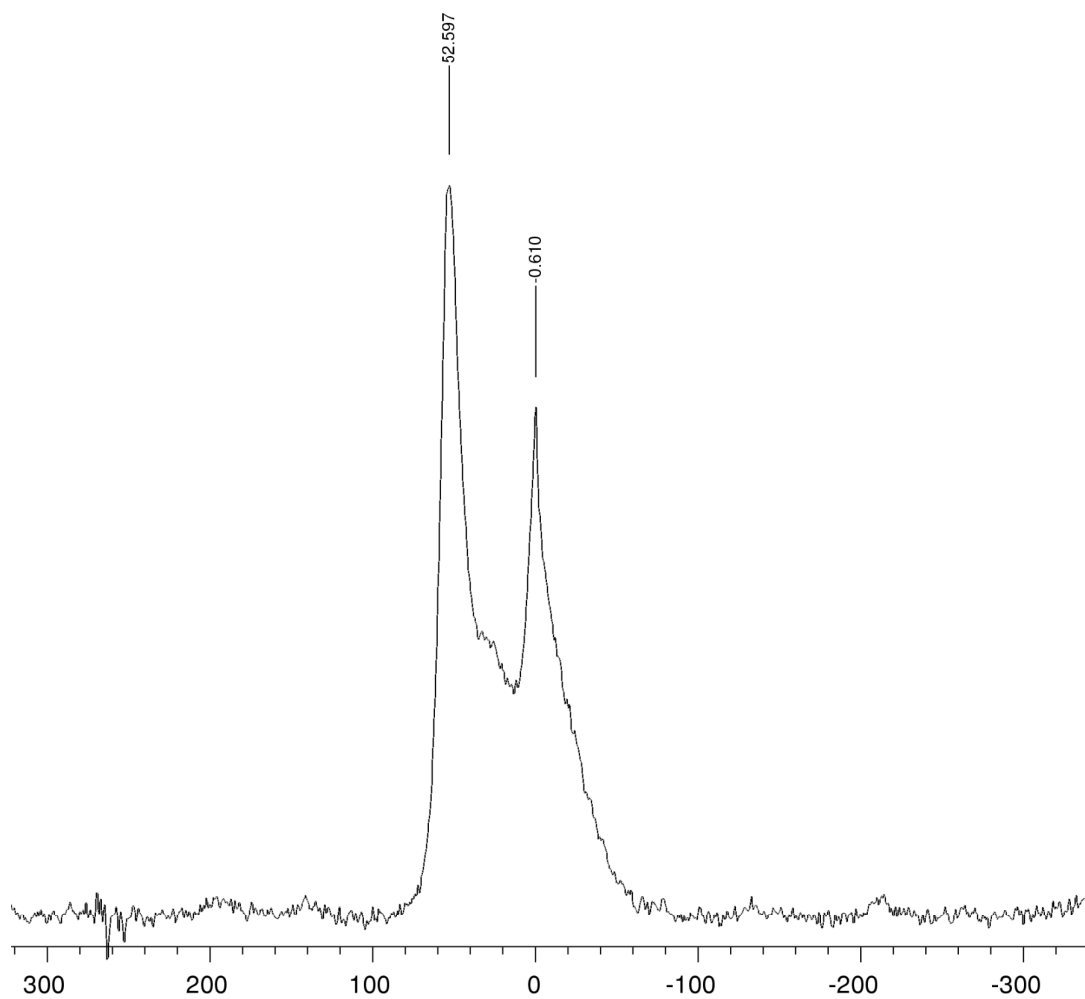


Figure S4b: ^{29}Si MAS NMR Al-13-(3.18)

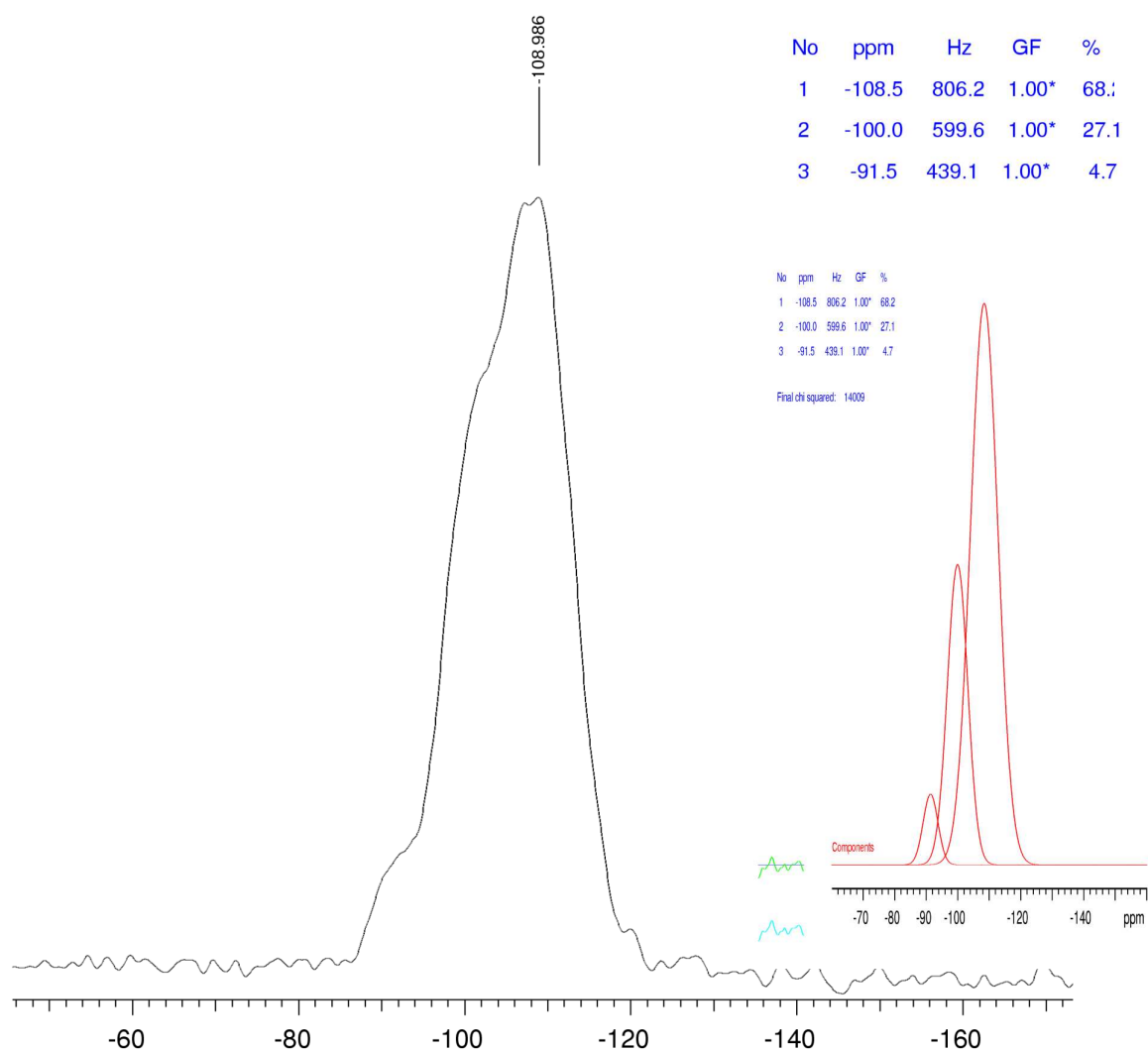


Figure S5: Al-13-(3.18) TPD Data

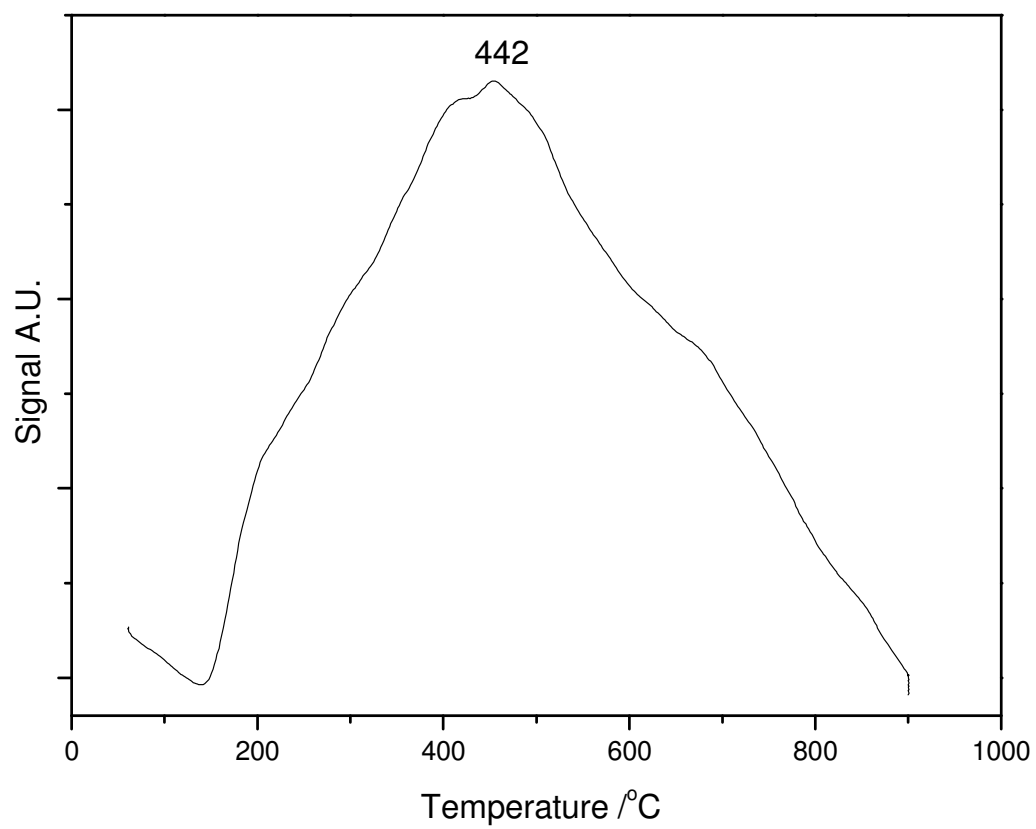


Figure S6: GC–MS Chromatogram of the Reaction of Glycerol with PMBA (2:1) Catalyzed by Al-13-(3.18) in DMC

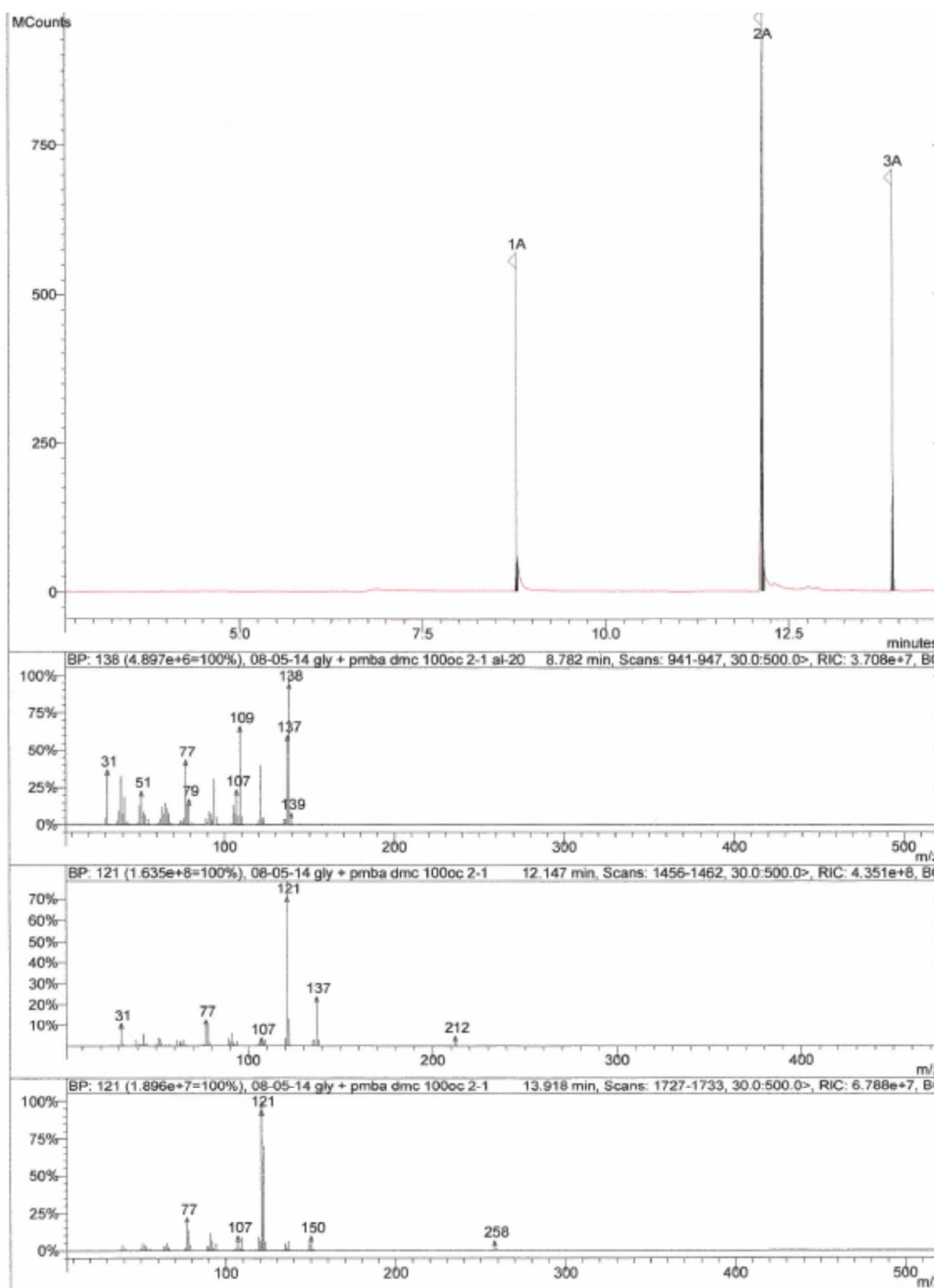


Figure S7: GC–MS Chromatogram of the Reaction of Glycerol with PMBA (2:1) Catalyzed by Amberlyst-15 in DMC

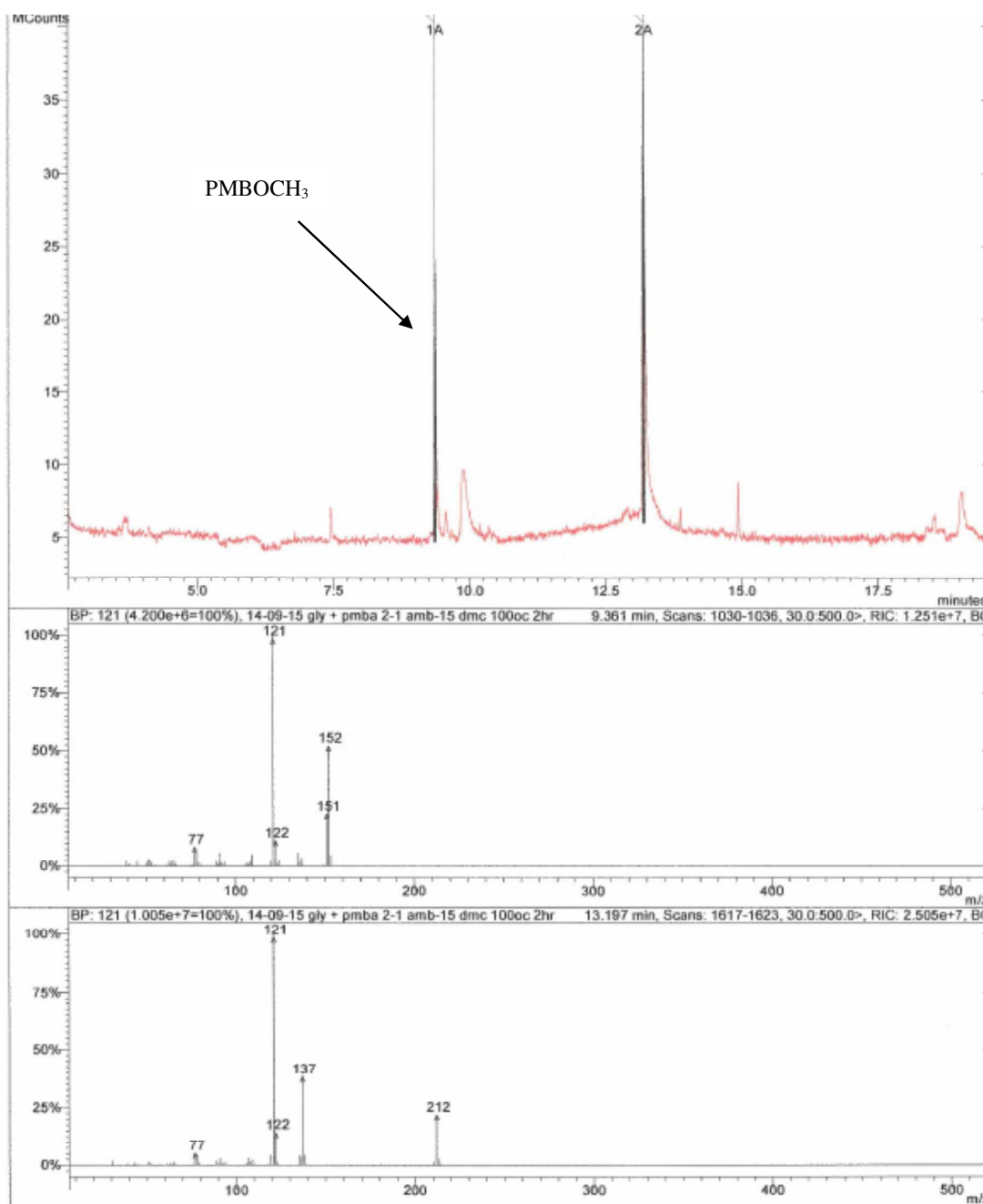
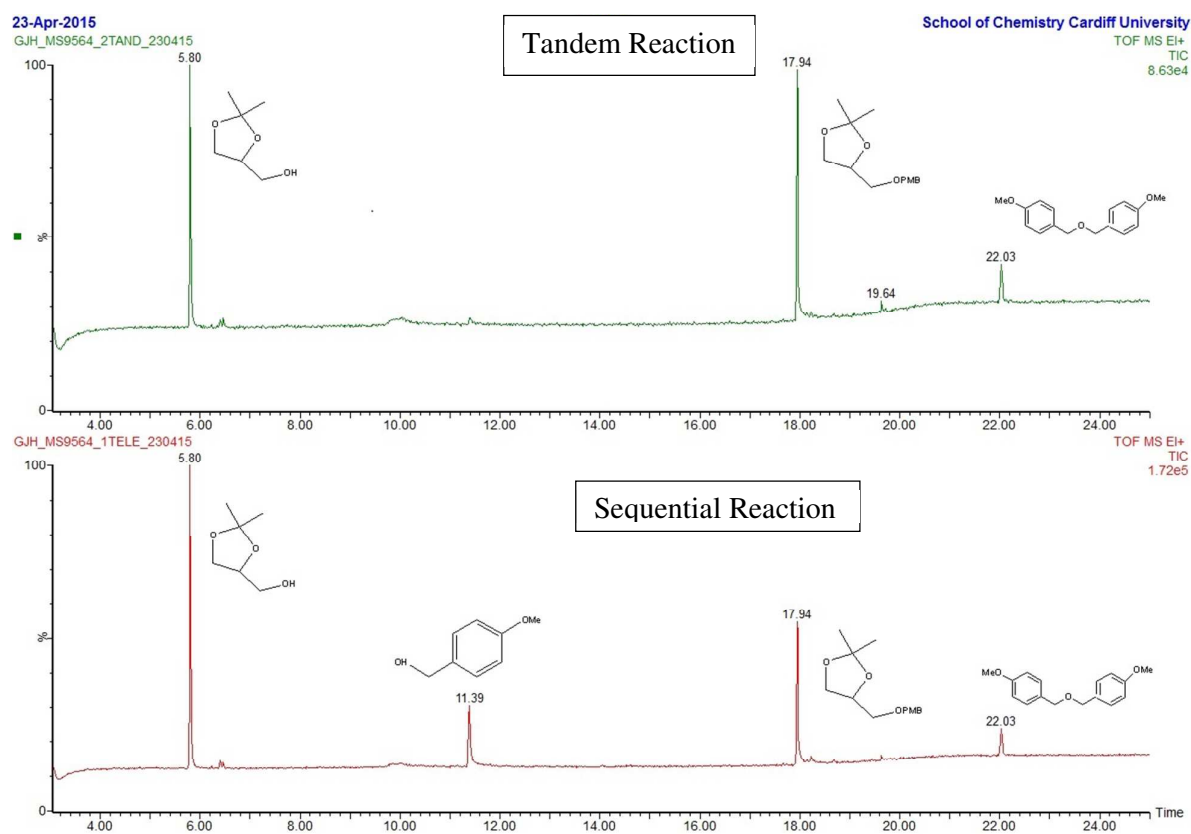


Figure S8: GC–MS Chromatograms of Telescoped Reactions of Glycerol with PMBA (4:1) Catalyzed by Al-13-(3.18) in Acetone



**Figure S9: GC–MS Chromatogram of the Sequential Reaction of Glycerol with PMBA (4:1)
Catalyzed by Amberlyst-15 in Acetone**

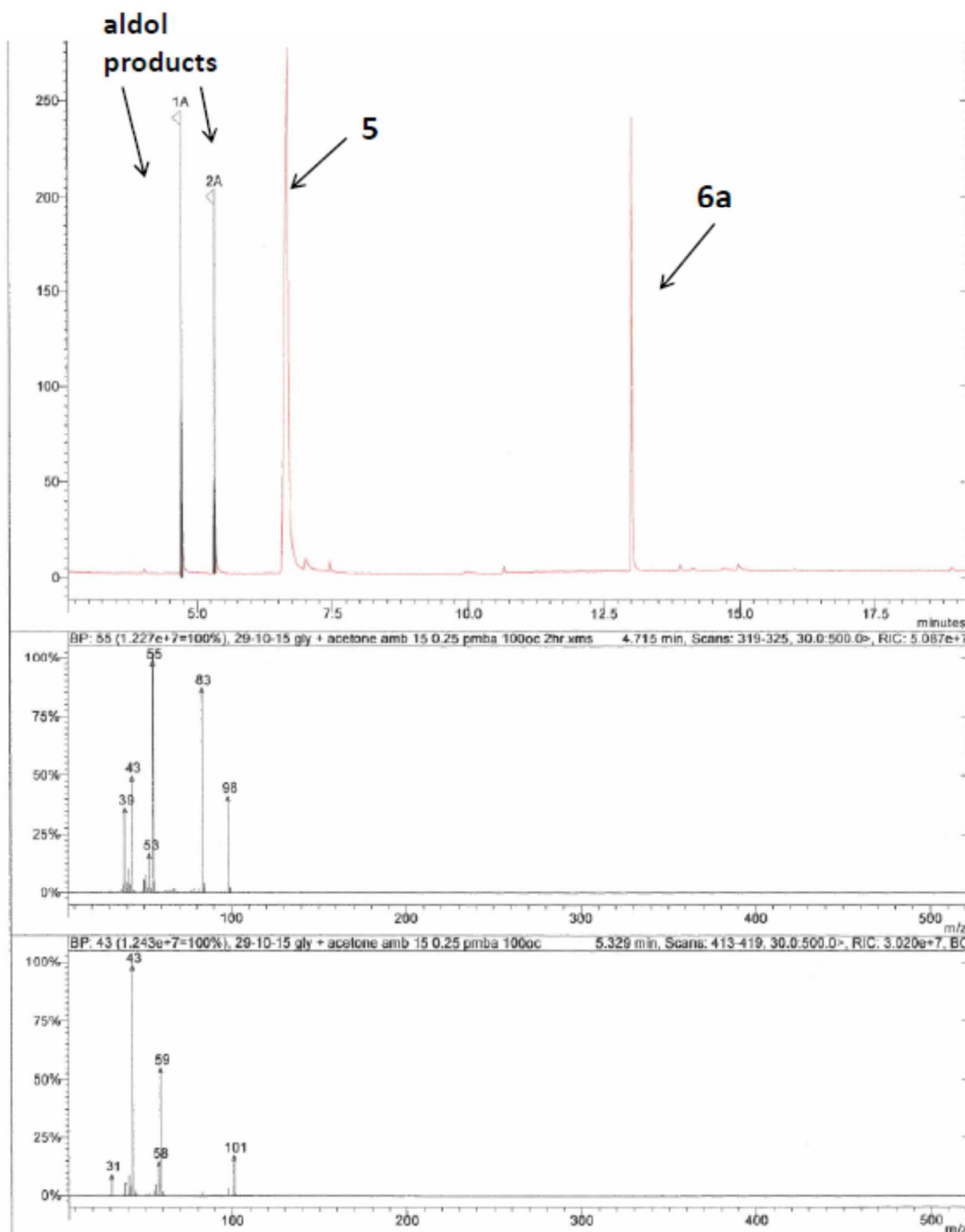
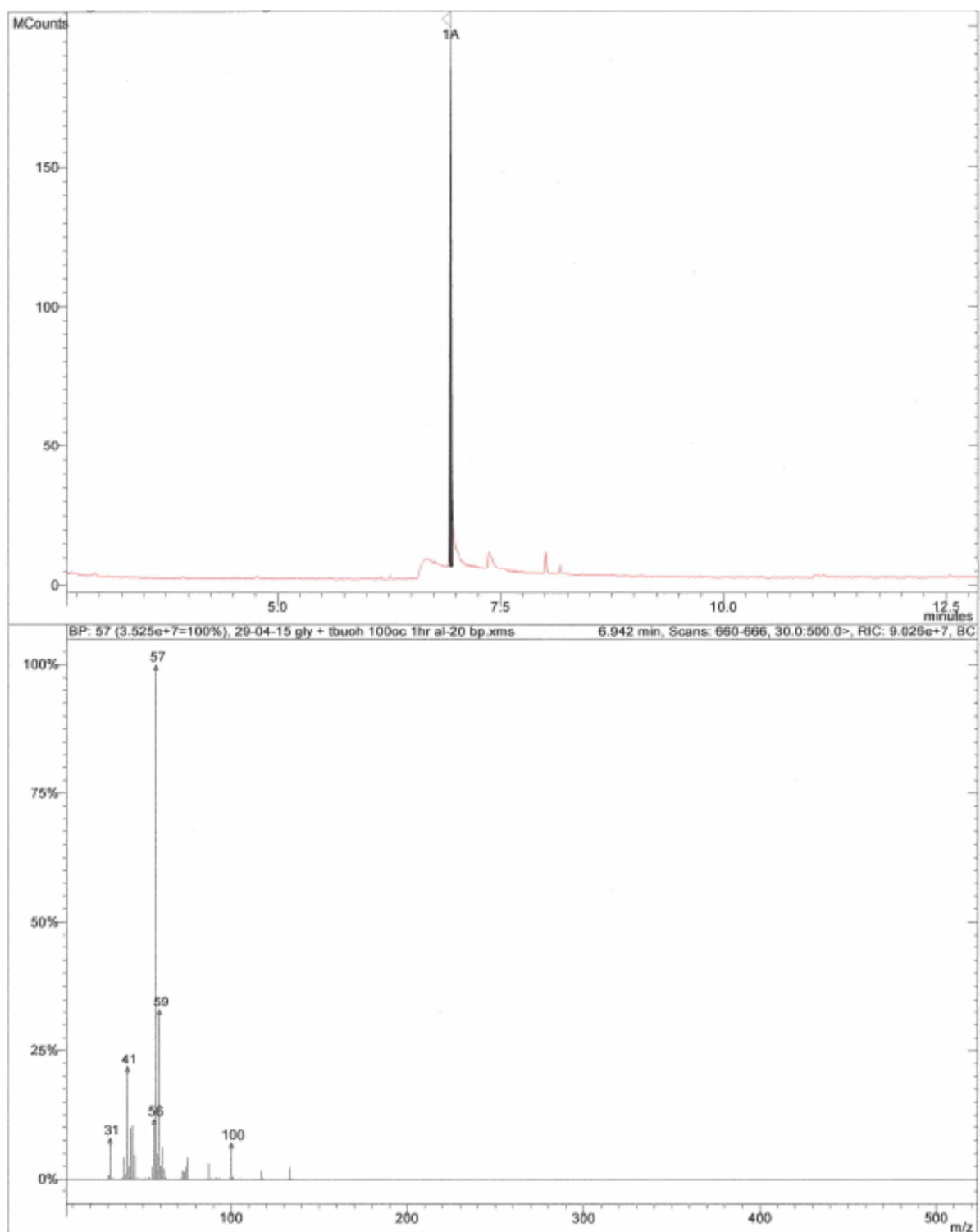


Figure S10: GC–MS Chromatogram of Crude Reaction of Glycerol with tert-BuOH Catalysed by Al-13-(3.18)



Spectroscopic Data for Ether Products

3-O-(4'-Methoxybenzyl)propane-1,2-diol (2a: Table 2, entry 2)⁵

¹H NMR (400 MHz, CDCl₃) δ = 7.25 (d, J = 8.0 Hz, 2H), 6.90 (d, J = 8.0 Hz, 2H), 4.50 (s, 2H), 3.85-3.90 (m, 1H), 3.80 (s, 3H), 3.70-3.75 (m, 1H), 3.65-3.70 (m, 1H), 3.55-3.60 (m, 1H), 3.50-3.55 (m, 1H), 2.55 (br s, 1H), 1.95 (br s, 1H); ¹³C NMR (100 MHz, CDCl₃) δ = 159.3, 129.8, 129.5, 113.9, 73.2, 71.4, 70.8, 64.0, 55.3; ν_{\max} (film)/cm⁻¹ (neat) 3401, 1613, 1513, 1248, 1034; MS (EI) m/z = 212 (M)⁺.

3-O-(4',4'-Dimethoxydiphenylmethyl)propane-1,2-diol (2b: Table 3, entry 5)

¹H NMR (400 MHz, CDCl₃) δ = 7.25 (d, J = 8.5 Hz, 4H), 6.90 (d, J = 8.5 Hz, 4H), 5.35 (s, 1H), 3.90-3.95 (m, 1H), 3.80 (s, 6H), 3.70-3.80 (m, 1H), 3.60-3.70 (m, 1H), 3.50-3.60 (m, 2H), 2.65 (br s, 1H), 1.65 (br s, 1H); ¹³C NMR (100 MHz, CDCl₃) δ = 159.1, 134.0, 128.1, 113.9, 83.6, 70.7, 70.5, 64.2, 55.3; ν_{\max} (film)/cm⁻¹ (neat) 3400, 1609, 1509, 1244, 1171, 1033; MS (EI) m/z = 318 (M)⁺; HRMS (CI) calculated for C₁₈H₂₂O₅Na (M + Na)⁺ 341.1360, found 341.1359.

3-O-(3,4-Dimethoxybenzyloxy)propane-1,2-diol (2c: Table 3, entry 7)⁶

¹H NMR (400 MHz, CDCl₃) δ = 6.85-6.90 (m, 3H), 4.50 (s, 2H), 3.90 (s, 3H), 3.89 (s, 3H), 3.50-3.80 (m, 5H), 2.75 (s, br, 1H), 2.10 (s, br, 1H); ¹³C NMR (100 MHz, CDCl₃) δ = 149.1, 148.3, 130.2, 120.5, 111.1, 111.0, 73.5, 71.6, 70.6, 64.1, 55.9, 55.8; ν_{\max} (film)/cm⁻¹ (neat) 3392, 1607, 1593, 1514, 1463, 1260, 1235, 1155, 1137, 1024; MS (EI) m/z = 242 (M)⁺.

3-O-(4',4'-Diphenylmethyl)propane-1,2-diol (2d: Table 3, entry 9)⁷

¹H NMR (400 MHz, CDCl₃) δ = 7.30-7.35 (m, 10H), 5.41 (s, 1 H), 3.55-4.05 (m, 5H), 2.55 (s, br, 1H), 2.05 (s, br, 1H); ν_{\max} (film)/cm⁻¹ (neat) 3376, 1493, 1452, 1073; MS (EI) m/z = 258 (M)⁺.

3-*tert*-Butoxypropan-1,2-diol (2f: Table 8, entry 1)⁸

¹H NMR (400 MHz, DMSO-d₆) δ = 4.50 (s, 1H), 4.45 (s, 1H), 3.35-3.40 (m, 2H), 3.25-3.30 (m, 2H),

3.15-3.20 (m, 1H), 1.15 (s, 9H); ^{13}C NMR (100 MHz, DMSO- d_6) δ = 72.9, 71.6, 63.8, 63.5, 27.8; ν_{max} (film)/ cm^{-1} (neat) 3420, 1191, 1073; MS (EI) m/z = 133 (M-15).

2,2-Dimethyl-1,3-dioxolane-4-methanol (Solketal) (5)⁹

CDCl_3

^1H NMR (400 MHz, CDCl_3) δ = 4.25-4.30 (m, 1H), 4.00-4.10 (m, 1H), 3.70-3.85 (m, 2H), 3.55-3.65 (m, 1H), 1.95 (br s, 1H), 1.70 (br s, 1H), 1.45 (s, 3H), 1.40 (s, 3H); ^{13}C -NMR (100 MHz, CDCl_3): δ = 109.4, 76.1, 65.7, 63.0, 26.7, 25.3; ν_{max} (film)/ cm^{-1} (neat) 3390, 1651, 1417, 1260, 1110, 1035; MS (EI) m/z = 117 (M-15).

DMSO- d_6

^1H NMR (400 MHz, DMSO- d_6) δ = 4.80 (t, J = 5.5 Hz, 1H), 4.00-4.10 (m, 1H), 3.90-4.00 (m, 1H), 3.60-3.65 (m, 1H), 3.40-3.50 (m, 1H), 3.30-3.40 (m, 1H), 1.30 (s, 3H), 1.25 (s, 3H); ^{13}C -NMR (100 MHz, DMSO- d_6): δ = 108.6, 76.6, 66.5, 62.6, 27.2, 25.9.

4-(4-Methoxybenzyloxymethyl)-2,2-dimethyl-1,3-dioxolane (6a: Table 4, entry 1)¹⁰

^1H NMR (400 MHz, CDCl_3) δ = 7.25 (d, J = 8 Hz, 2H), 6.85 (d, J = 8 Hz, 2H), 4.55 (s, 3H), 4.15-4.25 (m, 1H), 3.95-4.05 (m, 1H), 3.80 (s, 3H), 3.75-3.80 (m, 1H), 3.60-3.70 (m, 1H), 3.50-3.60 (m, 1H), 1.42 (s, 3H), 1.35 (s, 3H); ^{13}C -NMR (100 MHz, CDCl_3): δ = 159.3, 130.0, 129.4, 113.8, 109.4, 74.8, 73.2, 70.8, 66.9, 55.3, 26.8, 25.4; ν_{max} (film)/ cm^{-1} (neat) 1515, 1262, 1157, 1029; MS (EI) m/z = 252 (M)⁺.

4-(4,4'-Dimethoxydiphenyloxymethyl)-2,2-dimethyl-1,3-dioxolane (6b: Table 6, entry 1)

^1H NMR (400 MHz, CDCl_3) δ = 7.15 (d, J = 8.5 Hz, 4H), 6.80 (d, J = 8.5 Hz, 4H), 5.25 (s, 1H), 4.20-4.25 (m, 1H), 4.00-4.05 (m, 1H), 3.70-3.85 (m, 7H), 3.45-3.50 (m, 1H), 3.30-3.40 (m, 1H), 1.31 (s, 3H), 1.28 (s, 3H); ^{13}C -NMR (100 MHz, CDCl_3): δ = 158.9, 158.80, 134.4, 134.3, 128.2, 128.1, 113.8, 113.7, 109.30, 83.3, 74.8, 69.7, 55.3, 26.8, 25.5; ν_{max} (film)/ cm^{-1} (neat) 1609, 1508, 1462, 1442, 1370, 1242, 1170, 1080; MS (EI) m/z = 358; HRMS (CI) calculated for $\text{C}_{21}\text{H}_{26}\text{O}_5\text{Na}$ (M + Na)⁺

381.1673, found 381.1672.

4-(3,4-Dimethoxybenzyloxymethyl)-2,2-dimethyl-1,3-dioxolane (6c: Table 6, entry 2)⁶

¹H NMR (400 MHz, CDCl₃) δ = 6.85-6.95 (m, 3H), 4.50-4.55 (m, 2H), 4.30-4.35 (m, 1H), 4.05-4.10 (m, 1H), 3.91 (s, 3H), 3.90 (s, 3H), 3.80-3.85 (m, 1H), 3.70-3.75 (m, 1H), 3.50-3.60 (m, 1H), 3.45-3.50 (m, 1H), 1.45 (s, 3H), 1.38 (s, 3H); ¹³C-NMR (100 MHz, CDCl₃): δ = 149.0, 148.7, 130.5, 120.4, 111.0, 110.7, 109.4, 74.8, 73.4, 70.8, 66.7, 55.8, 26.8, 25.4; ν_{\max} (film)/cm⁻¹ (neat) 1515, 1464, 1420, 1370, 1261, 1157, 1087; MS (EI) m/z = 282.

4-(Diphenyloxymethyl)-2,2-dimethyl-1,3-dioxolane (6d: Table 6, entry 4)

¹H NMR (400 MHz, CDCl₃) δ = 7.25-7.35 (m, 10H), 5.45 (s, 1H), 4.35-4.40 (m, 1H), 4.10-4.15 (m, 1H), 3.85-3.90 (m, 1H), 3.60-3.65 (m, 1H), 3.50-3.55 (m, 1H), 1.42 (s, 3H), 1.39 (s, 3H); ¹³C-NMR (100 MHz, CDCl₃): δ = 143.0, 142.9, 128.4 ($\times 2$), 127.5 ($\times 2$), 127.0, 126.9, 109.3, 84.2, 74.8, 69.9, 67.1, 26.8, 25.5; ν_{\max} (film)/cm⁻¹ (neat) 1493, 1452, 1370, 1212, 1157, 1075; MS (EI) m/z = 298; HRMS (CI) calculated for C₁₉H₂₂O₃Na (M + Na)⁺ 321.1462, found 321.1461.

References

- 1) Kubczyk, T. M.; Williams, S. M.; Kean, J. R.; Davies, T. E.; Taylor, S. H.; Graham, A. E. *Green Chem.* **2011**, *13*, 2320–2325.
- 2) Robinson, M. W. C.; Davies, A. M.; Mabbett, I.; Davies, T. E.; Apperley, D. C.; Taylor, S. H.; Graham, A. E. *J. Mol. Catal. A: Chem.* **2010**, *329*, 57–63.
- 3) Robinson, M. W. C.; Davies, A. M.; Mabbett, I.; Davies, T. E.; Apperley, D. C.; Taylor, S. H.; Graham, A. E. *J. Mol. Catal. A: Chem.* **2009**, *314* 10–14.
- 4) T. E. Davies, J. R. Kean, D. C. Apperley, S. H. Taylor, A. E. Graham, *ACS Sustain. Chem. Eng.* **2014**, *2*, 860–866.
- 5) Qin, D.; Byun, H.-S.; Bittman, R. *J. Am. Chem. Soc.* **1999**, *121*, 662–668.
- 6) Alcaraz, M. L.; Peng, L.; Klotz, P.; Goeldner, M. *J. Org. Chem.*, **1996**, *61*, 192–201.
- 7) Gu, Y.; Azzouzi, A.; Pouilloux, Y.; Jérôme, F.; Barrault, J. *Green Chem.* **2008**, *10*, 164–167.
- 8) Jamróz, M. E.; Jarosz, M.; Witowska-Jarosz, J.; Bednarek, E.; Tęcza, W.; Jamróz, M. H.; Dobrowolski, J. C.; Kijęński, J. *Spectrochim. Acta A* **2007**, *67*, 980–988.

- 9) Yip, L.; Kubczyk, T. M.; Davies, T. E.; Taylor, S. H.; Apperley, D. C.; Graham, A. E. *Catal. Sci. Technol.* **2012**, 2, 2258–2263.
- 10) Lim, Z.-Y.; Thuring, J. W.; Holmes, A. B.; Manifava, M.; Ktistakis, N. T. *J. Chem. Soc. Perkin Trans. 1.* **2002**, 1067–1075.
- 11) Trikitiwong, P.; Sukpirom, N.; Shimazu, S.; Chavasiri, W. *Catal. Commun.* **2014**, 54, 104–107.